The EMBO Journal vol.13 no.10 pp.2247–2256, 1994

Crystal structure of a human rhinovirus neutralizing antibody complexed with a peptide derived from viral capsid protein VP2

José Tormo, Dieter Blaas, Nigel R.Parry[2], David Rowlands[2], David Stuart[3] and Ignasi Fita[4,5]

Institute of Biochemistry, University of Vienna, A-1090 Vienna, Austria, [2]Department of Molecular Sciences, Wellcome Research Laboratories, Beckenham, Kent BR3 3BS, [3]Laboratory of Molecular Biophysics, University of Oxford, Oxford OX1 3QU, UK and [4]Departement d'Enginyeria Química, Escola Tecnica Superior d'Enginyers Industrials, E-08028 Barcelona, Spain

[5]Corresponding author

Communicated by J.A.Subirana

The three-dimensional structure of the complex between the Fab fragment of an anti-human rhinovirus neutralizing antibody (8F5) and a cross-reactive synthetic peptide from the viral capsid protein VP2 has been determined at 2.5 Å resolution by crystallographic methods. The refinement is presently at an *R* factor of 0.18 and the antigen-binding site and viral peptide are well defined. The peptide antigen adopts a compact fold by two tight turns and interacts through hydrogen bonds, some with ionic character, and van der Waals contacts with antibody residues from the six hypervariable loops as well as several framework amino acids. The conformation adopted by the peptide is closely related to the corresponding region of the viral protein VP2 on the surface of human rhinovirus 1A whose three-dimensional structure is known. Implications for the cross-reactivity between peptides and the viral capsid are discussed. The peptide–antibody interactions, together with the analysis of mutant viruses that escape neutralization by 8F5 suggest two different mechanisms for viral escape. The comparison between the complexed and uncomplexed antibody structures shows important conformational rearrangements, especially in the hypervariable loops of the heavy chain. Thus, it constitutes a clear example of the 'induced fit' molecular recognition mechanism.

Key words: antibody structure/cross-reactivity/crystal structure/human rhinovirus/viral neutralization

Introduction

Human rhinoviruses (HRVs), members of the picornavirus family, are small, icosahedral RNA viruses and are the main causative agent of the common cold. The capsid of all picornaviruses is composed of 60 copies of each of four proteins, VP1, VP2, VP3 and VP4, arranged on a T = 1 icosahedral surface (Rossmann and Johnson, 1989). The three large capsid proteins VP1–VP3 share a common core structural motif, an eight-stranded β-barrel. The secondary structural elements of this barrel are connected by loops, of dissimilar length and structure, that decorate the surface of the virus. Binding sites for neutralizing antibodies are generally located in these hypervariable loops and flank the 'canyon' which has been shown to contain the recognition site for the receptors of HRVs (Olson *et al.*, 1993). Three neutralizing antigenic sites, designated A, B and C, have been defined for HRV2 by analysis of escape mutants (Appleyard *et al.*, 1990) and by using structural information available for a closely related serotype, HRV1A (Kim *et al.*, 1989). Although the antigenic properties of rhinoviruses and other picornaviruses have been extensively studied, our understanding of the molecular mechanisms of viral neutralization by antibodies and viral escape from the immunological surveillance of the host is limited (Dimmock, 1993). Cryoelectron microscopy has provided low resolution images of the interaction between antibodies and several icosahedral viruses (Prasad *et al.*, 1990; Wang *et al.*, 1992; Smith *et al.*, 1993) but no detailed structural information of atomic detail for these large macromolecular complexes is available. In this work we report the three-dimensional structure of the complex between a synthetic peptide which constitutes a continuous epitope on the surface of the viral protein VP2 and the Fab fragment from a monoclonal antibody (8F5) that neutralizes HRV2, determined by X-ray crystallography at 2.5 Å resolution. This structure is compared with the conformation of the uncomplexed 8F5 antibody which has been solved at 2.8 Å resolution in our laboratory (Tormo *et al.*, 1992).

The antibody 8F5, raised against native virions, not only binds to the viral particle in its native conformation, but also to the viral protein VP2 on Western blots (Skern *et al.*, 1987). This allowed the region of the binding site to be defined, by bacterial expression of various deletion mutants of VP2, as lying between residues 2153 and 2164 (in this nomenclature the first digit indicates the viral capsid protein, here VP2). This polypeptide segment is located in the region of site B, analogous to the NIm-II antigenic site on HRV14 (Rossmann *et al.*, 1985). As antibody 8F5 also recognizes peptides bearing this sequence, an extensive analysis of the recognition site was carried out with a set of overlapping peptides (Hastings *et al.*, 1990). These experiments defined the minimal binding site as the sequence TRLNPD corresponding to residues 2160–2165, although residues AE (2158–2159) also contribute significantly to the binding. The 15-mer synthetic peptide used in our study has the sequence (VKAETRLNPDLQPTE-NH_2) corresponding to residues 2156–2170. It thus includes the minimal binding site of 8F5, as well as all those residues whose mutations give rise to escape neutralization by this antibody (Appleyard *et al.*, 1990; N.R.Parry and D.Rowlands, unpublished results). This peptide has also been used to raise peptide-specific antisera which both bind to and neutralize HRV2 (Francis *et al.*, 1987; Hastings *et al.*, 1990).

There is much interest in deciphering the molecular basis of the antigenic cross-reactivity of antibodies. Anti-peptide antibodies which cross-react with its cognate protein antigen

have been extensively used for the mapping of protein epitopes (Geysen *et al.*, 1987; Van Regenmortel, 1989). When applied to the mapping of epitopes on proteins from pathogens, immunization with synthetic peptides has given rise to neutralizing antibodies in several examples: diphtheria (Audibert *et al.*, 1982), cholera (Jacob *et al.*, 1984), malaria (Patarroyo *et al.*, 1988), common cold (Francis *et al.*, 1987; Hastings *et al.*, 1990), influenza (Muller *et al.*, 1982), foot-and-mouth disease (Parry *et al.*, 1989) and HIV (Javaherian *et al.*, 1990; Rini *et al.*, 1993). These encouraging results have increased the prospect of constructing synthetic peptide vaccines against many viral, bacterial and parasitic diseases.

Results and discussion

Overall structure

The overall architecture of the four structural domains (variable heavy, variable light, constant heavy and constant light) of Fab 8F5 in its complex with the viral peptide, as well as the relationships between these domains, are similar to those previously reported (reviewed by Amzel and Poljak, 1979; Alzari *et al.*, 1988). The main chain conformations adopted in the complex by five of the six hypervariable regions are the same canonical models (Chothia *et al.*, 1989) found in the unbound 8F5 Fab structure (Tormo *et al.*, 1992). The conformations of hypervariable loops H3 (for which no canonical forms have been proposed) are also closely related in both 8F5 structures, with a root mean square (r.m.s.) deviation for main chain atoms superposition of 0.6 Å. Nonetheless, there are substantial structural differences between the bound and unbound Fab 8F5 which will be analyzed below.

The crystal structure of the complex reported in this work comprises 431 residues from the Fab fragment (221 residues from the light chain and 210 from the heavy chain), the whole synthetic peptide (15 residues) and ~50 solvent molecules. The Fab residues presently missing in the model are GluH1–ValH2 and GlyH134–GlyH138 [residue numbers for heavy and light chain amino acids are preceded by H or L, respectively; the complementarity-determining regions (CDR) are also indicated when appropriate]. The two first residues of the heavy chain present very weak density and are probably disordered. These amino acids showed good density in the unliganded Fab structure where they contacted residues from CDR-H1 and CDR-H3. The disorder in this region can be related to the displacement of these loops in the structure of the peptide complex (see below). Density corresponding to residues GlyH134–GlyH138 is also weak . These residues form a solvent exposed loop between two adjacent β-strands in the constant heavy domain and were also disordered in the unbound Fab structure. The residue starting this loop, CysH133, participates in the unique interchain disulfide bridge with the last residue of the light chain, CysL220. Density for side chains from residues GluL160 to AsnL163, situated in a solvent accesible loop of the constant light domain, is also poor.

Electron density around the antigen-binding site is well defined, including the long loop on CDR-L1 that presented weak density for its side-chains and high temperature factors in the unbound Fab structure, but which is much more ordered in the peptide–Fab complex, probably because it establishes contacts with the antigen. The electron density map for the main and side chains of most peptide residues is also clear (Figure 1). High temperature factors and poor density for the N-terminal (Val2156) and C-terminal (Thr2169–Glu2170) peptide regions indicate flexibility of those residues.

All peptide and Fab residues but one, AlaL57, are inside or very near to energetically allowed regions in the Ramachandran diagram. AlaL57 (ϕ = 67.2°, ψ = −29.3°) belongs to CDR-L2 which adopts (ϕ, ψ) values characteristic of a type I′ or ($\gamma\gamma$) β-turn (Richardson, 1981; Wilmot and Thornton, 1990).

Peptide structure

The peptide structure found in this complex has a compact folded conformation (Figure 2), the C_α atoms of residues

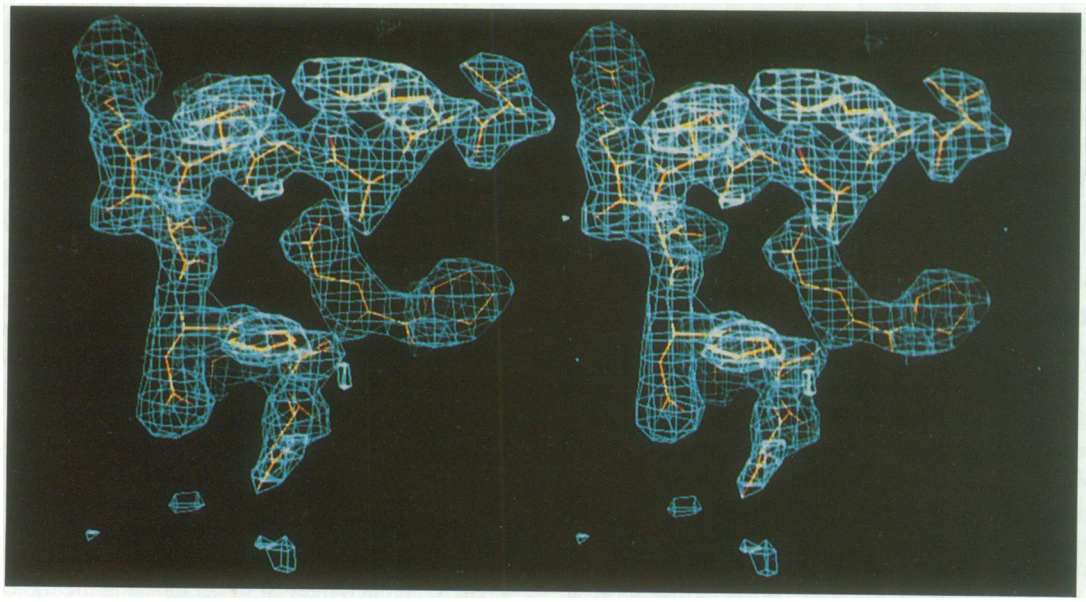

Fig. 1. Stereo view of an (F_o–F_c) omit map (in blue) of the peptide at 2.5 Å resolution. The peptide model placed inside the density is also shown for clarity. The figure was displayed using the program TOM (Cambillau and Horjales, 1987) on an IRIS Silicon Graphics workstation.

Lys2157 and Gln2167 are only 6.9 Å apart. Different kinds of turns are observed. There is a γ-turn between residues Ala2158 and Thr2160; residues Ala2158–Arg2161 adopt a type I or ($\alpha\alpha$) β-turn conformation; and, finally, the side chain of Asn2163 is hydrogen bonded to the backbone amino group of Asp2165 forming what has been called an Asn-pseudoturn. Asn2163 can also be considered as the N-cap residue of a short 3_{10} helix formed by residues Pro2164–Gln2167. The folded conformation of the peptide is further stabilized by several side chain–side chain and side chain–main chain intrapeptide interactions. Thus, Glu2159 and Arg2161 form a lateral salt bridge whereas the side chain of Gln2167 loops backwards making two well defined hydrogen bonds with main chain atoms of residue Glu2159. Pro2168 has been built in *cis* conformation.

Peptide–antibody interactions

The arrangement of the CDR loops in Fab 8F5 creates a cavity occupied by the peptide in the complex (Figure 2). The interaction between antigen and antibody is very extensive. The contact surface areas, calculated using the program MS (Connolly, 1983) with a 1.7 Å probe radius and standard van der Waals radii (Case and Karplus, 1979), were 795 Å^2 on the peptide and 945 Å^2 on the Fab fragment. These values are similar to those found for antibody–protein complexes (between 680–899 Å^2 for the protein antigen and 690–916 Å^2 for the antibodies) and larger than the buried surfaces reported for Fab–peptide complexes (between 468–725 for the Fab and 436–620 for the peptide antigen), although fewer amino acids, between seven and nine, were included in those peptide models (for reviews see Davies *et al.*, 1990; Wilson and Stanfield, 1993). The structure of the cyclosporin A–Fab complex constitutes an intermediate example with a buried surface area for the Fab (577 Å^2) comparable with other peptide–Fab complexes, whereas the area for the peptide (811 Å^2) is well inside the range reported for protein–Fab complexes (Vix *et al.*, 1993). The 8F5 Fab surface in direct

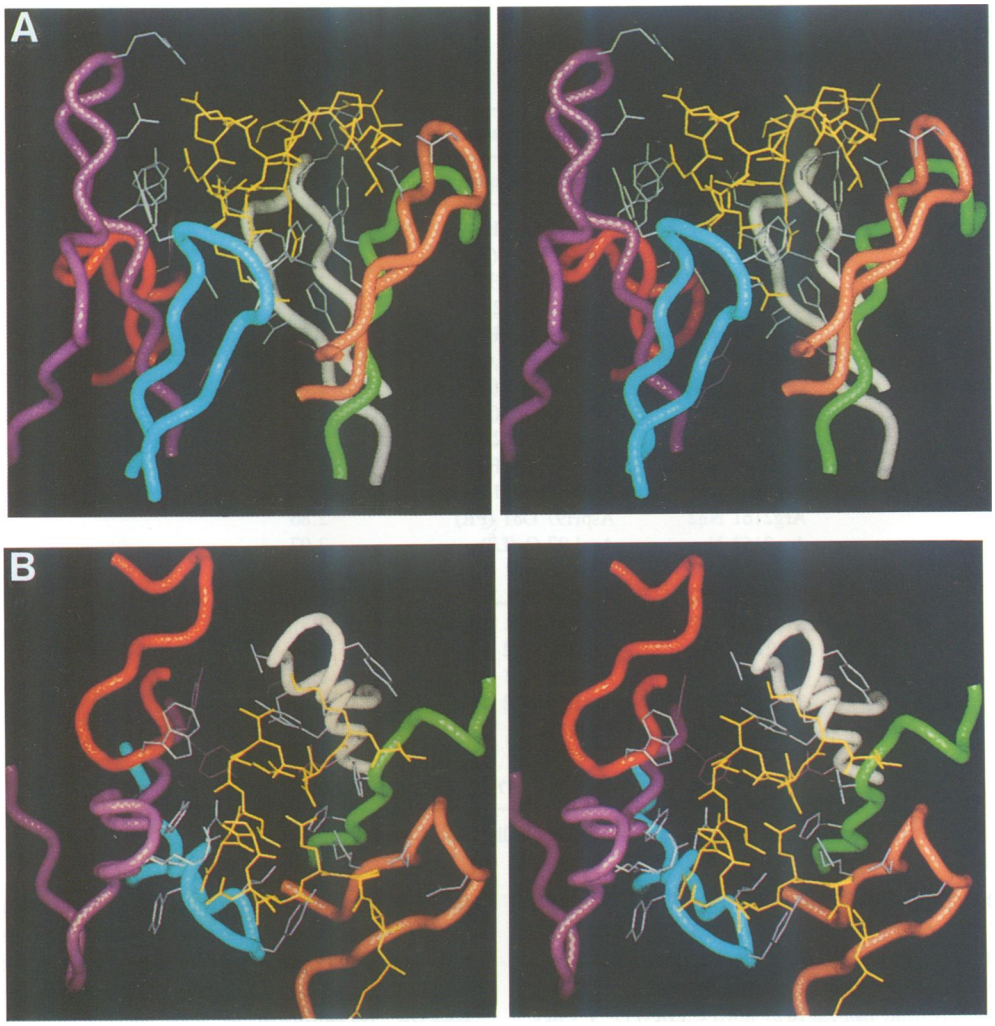

Fig. 2. Stereo view of the binding pocket of the Fab 8F5–peptide complex. (**A**) Side view and (**B**) upper view showing the synthetic peptide from the viral capsid protein VP2 in yellow, side chains of CDR residues which show extensive contacts with the antigen in gray and side chains of framework residues in violet. The main chain backbones of the six CDRs are shown in different colors. The three hypervariable loops from the light chain are on the left (CDR-L1, magenta; CDR-L2, red; CDR-L3, blue) and those belonging to the heavy chain are on the right (CDR-H1, green; CDR-H2, orange; CDR-H3, white). In (B), the N-terminal residue of the peptide (Val2156) is in the upper right side contacting CDR-H1, whereas the C-terminal residue (Glu2170) is at the lower right side contacting residues from CDR-H2. The type-I β-turn and Asn-pseudoturn, which confer to the peptide its folded conformation, are respectively at the upper and lower left sides of the combining site. The figures were made with the program 'O' (Jones *et al.*, 1991) on an Evans and Sutherland graphics workstation.

Table IA. Contacts[a] between the peptide and the Fab in the complex

HRV2 peptide			Fab fragment from antibody 8F5
Residue	Atoms	Contacts	Residues and number of contacts
Val2156	2	2	LysH30(1) TyrH33(1)
Lys2157	8	21	TyrH33(3) SerH101(12) TyrH102(5) AspH104(1)
Ala2158	2	2	SerH101(2)
Glu2159	7	26	TyrH33(16) HisH35(3) ArgH50(3) TyrH99(4)
Thr2160	6	15	TyrL55(1)[b] TrpL56(5) TyrH99(5) SerH101(10) AspH104(3)
Arg2161	8	23	TyrL38(1) Tyr42(1)[b] LeuL52(1)[b] TyrL55(1)[b] AsnL97(3) HisH35(3) AspH97(4)[b] TyrH99(6) AspH106(3)
Leu2162	3	8	TyrL38(2) AsnL97(5) LeuL102(1)
Asn2163	6	16	AsnL31(3) TyrL38(6) AsnL97(2) TyrL98(5)
Pro2164	2	4	ArgL33(1) TyrL38(3)
Asp2165	3	3	AsnL31(3)
Leu2166	4	10	TyrL98(2) AsnL99(3) TyrL100(5)
Gln2167	1	1	ArgH50(1)
Pro2168	2	2	AspH52(2)
Thr2169	5	6	AspH52(3) AsnH55(1) TyrH57(2)
Glu2170	9	14	TyrH57(4) ThrH122[c](1) AlaH123[c](7) ThrH209[c](1) ProH124[c](1)

[a]Contact distances were taken from Sheriff *et al.* (1987).
[b]Framework residues.
[c]Residues from a crystallographically related molecule.

Table IB. Hydrogen bonds between the peptide and the Fab

Peptide	8F5 Fab fragment	Distance (Å)
Lys2157 O	TyrH33 Oη (H1)	2.89
Lys2157 O	SerH101 Oγ (H3)	2.83
Lys2157 Nζ	SerH101 O (H3)	2.43
Lys2157 Nζ	AspH104 Oδ2 (H3)	3.00
Glu2159 Oε1	ArgH50 Nε (H2)	2.84
Glu2159 Oε1	ArgH50 Nη2 (H2)	2.88
Glu2159 Oε2	HisH35 Nε2 (H1)	2.90
Thr2160 O	TrpL56 Nε1 (L2)	2.93
Thr2160 Oγ1	AspH104 Oδ2 (H3)	2.68
Arg2161 Nη1	TyrL42 Oη (FR)	3.02
Arg2161 Nη1	AspH106 Oδ1 (H3)	3.17
Arg2161 Nη2	AspH97 Oδ1 (FR)	2.86
Asn2163 N	AsnL97 O (L3)	3.07
Asn2163 Oδ1	AsnL31 Nδ2 (L1)	2.54
Asn2163 Nδ2	TyrL98 O (L3)	2.91
Asp2165 Oδ2	AsnL31 Nδ2 (L1)	3.37
Gln2167Oε1	ArgH50 Nη2 (H2)	3.32
Thr2169 N	AspH52 Oδ1 (H2)	2.99
Thr2169 O	AsnH55 Nδ2 (H2)	2.86
Glu2170 NT	ProH124[a] O	3.04
Glu2170 Oε1	AlaH123[a] N	2.96
Glu2170 Oε2	ThrH122[a] Oγ1	3.32

[a]Residues from a crystallographically related molecule

contact with the peptide comprises the six CDR loops and five framework residues (Table IA); 12 residues are from the light chain (among them three framework residues) and 14 from the heavy chain (two framework residues). The antigen shows preferential interaction with CDR-H2, CDR-H3 and CDR-L3; whereas CDR-L2 contributes only 3.5% to the total number of contacts (Figure 3). All the amino acids from the peptide are directly involved in interactions with the antibody. As shown in Figure 3, the contribution of the different hypervariable loops and peptide amino acid residues to the peptide–antibody interactions depends notably on the method used to analyze them (accessible surface area buried upon complex formation, and van der Waals contacts). A diversity of hydrogen bonds between the Fab and the peptide (Table IB), some of them with ionic character, indicates that polar interactions are important for specific recognition in this antigen–antibody complex. Interestingly, framework residues (TyrL42 and AspH97) are making hydrogen bonds with the peptide Arg2161 side chain. Carboxylate groups of AspH97 and AspH106 in the unliganded Fab structure were proposed (Tormo *et al.*, 1992) to define a suited pocket to bind the guanidinium group of Arg2161 and this has now been confirmed in the complex (Figure 4).

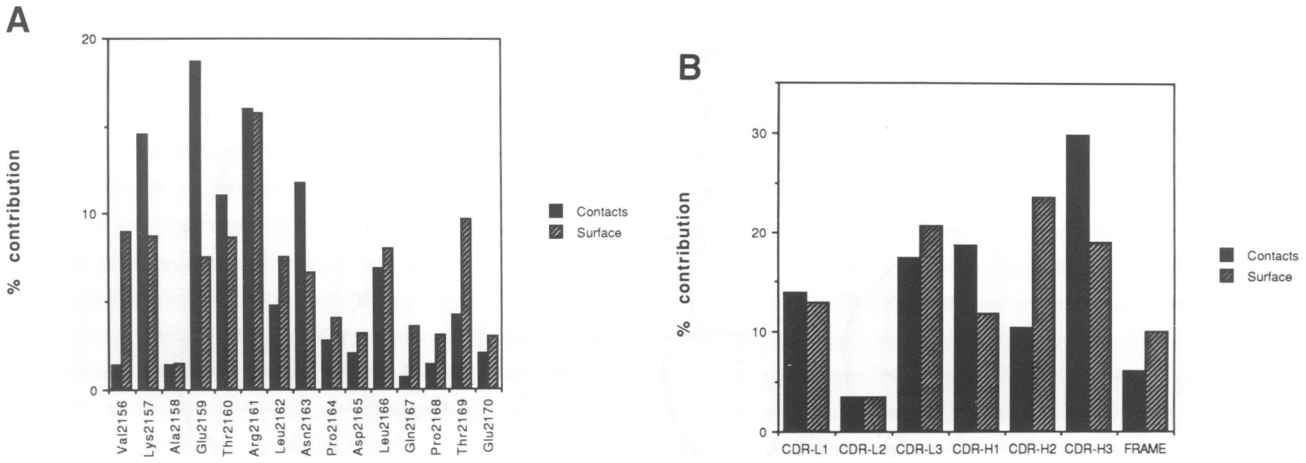

Fig. 3. Buried area and number of contacts expressed as the percentage of the total. In (**A**) for the 15 peptide residues and in (**B**) for the six hypervariable loops and framework residues.

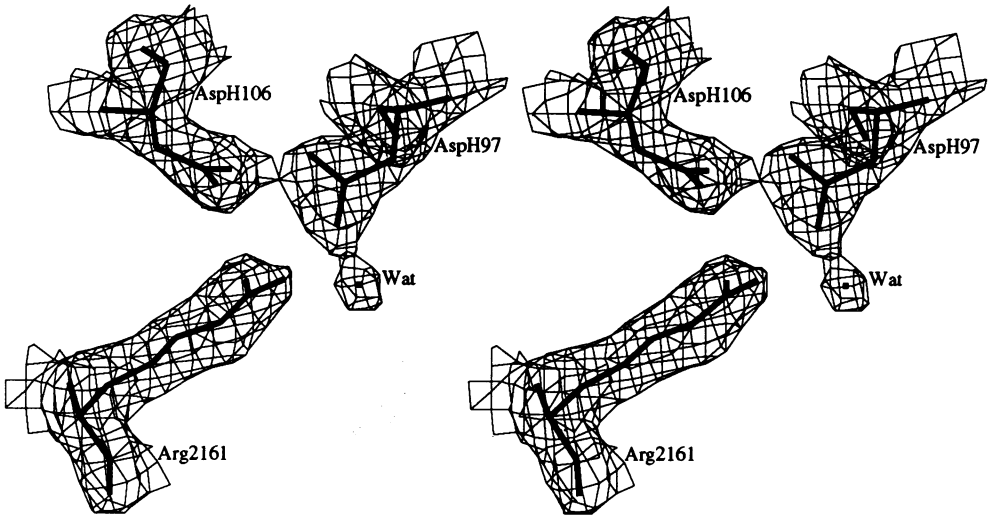

Fig. 4. Stereo plot of the peptide residue Arg2161 and the amino acids from the Fab heavy chain AspH97 and AspH106. The corresponding electronic density in a $2F_o-F_c$ map is also shown. The proximity of the two carboxylate groups suggests that at least one of them must still be protonate (as was also observed in the structure of the unbound 8F5) in spite of the interaction with the guanidinium group of Arg2161. A water molecule in the close vicinity of AspH97 is included in this drawing.

Aromatic residues located in the antigen-binding site of antibody 8F5 contribute to 55% of the total van der Waals contacts between antigen and antibody. The high frequency of aromatic residues in the ligand binding site of immunoglobulins and histocompatibility proteins has been described previously (Bjorkman *et al.*, 1987; Padlan, 1990; Mian *et al.*, 1991). In the peptide–8F5 complex, besides hydrogen bonds formed by the hydroxyl group of tyrosines and the nitrogen atom in the indole side chain of tryptophans, the aromatic rings mainly participate in non-polar interactions. However, a few of the contacts involving atoms from aromatic rings could be classified as weak polar interactions (Burley and Petsko, 1988). Thus the side chain amide group of Asn2163 points towards the center of the aromatic ring of TyrL98(CDR-L3). The positive partial charge of the hydrogen on the amide group can interact favorably with the negative partial charge of the π-electron cloud of the aromatic ring. An example of an oxygen–aromatic interaction can be found in the backbone carbonyl group of Arg2161 which is located in the plane of the aromatic ring of TyrL38(CDR-L1) at 3.5 Å from one of the carbon atoms of the ring.

The analysis of interactions shows that, although peptide residues forming a β-turn (Glu2159–Leu2162) buried in the antigen binding 1pocket dominate the interaction with antibody, a feature which appears to be common to most of the known structures of peptide–antibody complexes (Stanfield *et al.*, 1990; Garcia *et al.*, 1992; Rini *et al.*, 1992), there are also extensive contacts, mainly through hydrogen bonds, between backbone atoms throughout all the peptide and the antibody combining site, resembling the interactions observed in antibody–protein complexes (Davies *et al.*, 1990).

The number of contacts in the peptide amino acid residues (Figure 3) correlates well with epitope mapping results from earlier immunological studies (Skern *et al.*, 1987; Hastings *et al.*, 1990) which showed that the minimal binding site was included between residues Ala2158 and Asp2165 (AETRLNPD). This sequence contains most of the residues that contribute >10% to the contact surface area (Glu2159,

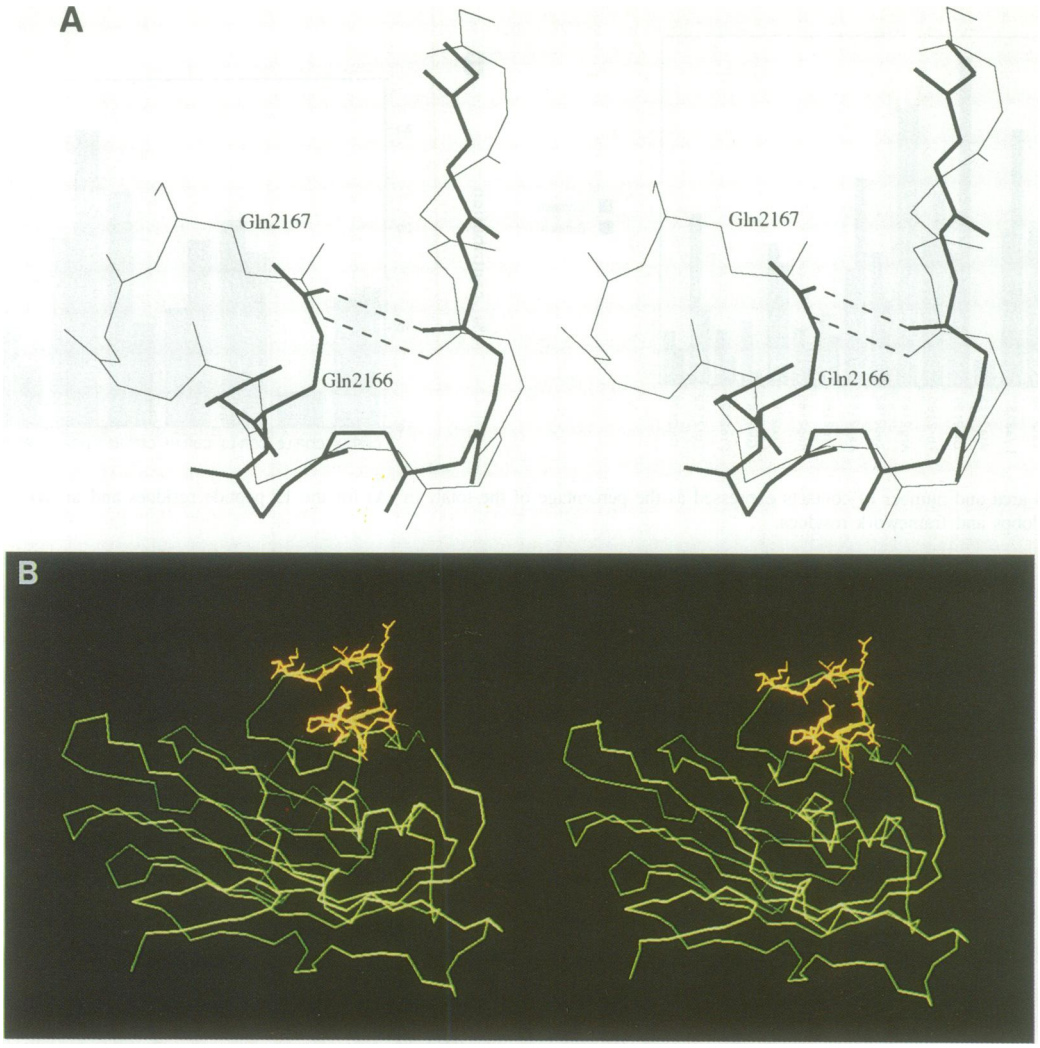

Fig. 5. (**A**) Stereo plot of the superposition of the structure determined in this work for the HRV2 peptide, residues Ala2158–Gln2167 (thin line), with the equivalent residues in the structure of HR1A. The superimposition was performed according to the highest structural homology found between the peptide and VP2 in HRV1A. Only main chain atoms and the intrapeptide hydrogen bonded side chains of Gln2166 (from HRV1A) and Gln2167 (from the peptide) are shown. Hydrogen bonds are drawn as discontinuous lines. Residues Pro2164–Asp2165–Leu2166 in HRV2 form a short 3_{10} helix and appear as an insertion with respect to the HRV1A sequence (see text). (**B**) Location of the superimposed peptide (yellow) on the homologous region of VP2 from HRV1A (green) (Kim *et al.*, 1989). The figure was displayed using the program TOM (Cambillau and Horjales, 1987) on a IRIS Silicon Graphics workstation.

18.7%; Thr2160, 11.1%; Arg2161, 16.0%; Asn2163, 11.8%). Only Lys2157, which contributes 14.6% to the total number of contacts, was not found to be essential for peptide binding in those studies.

Structural relationship between the peptide antigen and the cognate sequence on the surface of the virus

Antibody 8F5 was raised against intact virions. To what extent is the peptide structure related to the conformation adopted by VP2 in the intact virion? The three-dimensional structure of HRV2 has not yet been determined. Therefore the atomic coordinates of HRV1A (Kim *et al.*, 1989), which is closely related to HRV2, were used in the search for structural homologies. The least squares superposition of C_α atoms from residues 2157 to 2164 in the peptide with residues 2159–2166 in HRV1A gives an r.m.s. of 0.9 Å. The corresponding r.m.s. for C_β atoms between equivalent residues is 1.4 Å. Thus, both main chain atoms and side chain orientations, for those residues, can be closely superimposed (Figure 5). This alignment implies an insertion of three residues (Pro2164–Asp2165–Leu2166 in HRV2) and a deletion of two residues (Ser2157–Gln2158) with respect to HRV1A (Table II). The side chains of Gln2167 in HRV2 and Gln2166 in HRV1A appear to play structurally equivalent roles, making hydrogen bonds with peptide groups at the beginning of the loop (Figure 5A). Whereas Pro2168 in the peptide has a *cis* conformation Pro2167 in HRV1A has adopted a *trans* conformation. As a consequence residues Thr2169–Glu2170 in the peptide and Ser2168–Asp2169 in HRV1A progressively diverge in this structural alignment. The most obvious sequence alignment (Kim *et al.*, 1989), requiring only a single insertion in HRV2 with respect to HRV1A, gives a poor structural superimposition (r.m.s. deviation of 3.5 Å for the C_α atoms of residues Lys2157–Pro2164). This structural homology suggests: first, that this large loop of VP2 presents similar folding in both serotypes, HRV1A and HRV2, even though these regions do not show any detectable sequence similarity and also differ in length, and second that the peptide antigen partially mimics the conformation of the corresponding

Table II. Sequence alignments and amino acid substitutions for HRV1A and HRV2

HRV1A	2153	G R D V S Q E R D A S L R – – – Q P S D D S W	2172
HRV2	2153	G R E V – – K A E T R L N P D L Q P T E E Y W	2173
		↓ ↓ ↓ ↓	
HRV2 escape mutant		G T Y S	
		S	

Sequence alignment of HRV1A and HRV2 around the continuous epitope recognized by antibody 8F5, based on the structural equivalences discussed in this work. Shown below the sequences are amino acid substitutions which give rise to HRV2 mutant viruses that escape neutralization by antibody 8F5 (Appleyard *et al.*, 1990; N.R.Parry and D.Rowlands, unpublished data).

epitope in the intact protein on the surface of the virus. The ability of the peptide to adopt a three-dimensional arrangement at least partially equivalent to an extensive part of a probably more complex epitope explains the cross-reactivity between peptide and viral particle.

The combination of the detailed knowledge on the stereochemistry of the peptide–antibody interactions together with the analysis of a series of neutralization escape mutants (Table II) gives support to two different mechanisms for escape from neutralization. The mutations Glu2159Gly and Arg2161Thr disrupt strong salt bridges between the side chains of these residues and antibody amino acids located in a deep cavity in the antigen binding site. On the other hand, Pro2164 does not interact extensively with the antibody and its substitution for Ser may result in escape from neutralization by causing the destabilization of the short 3_{10} helix, and triggering local rearrangements in the structure of the loop. For the remaining residue, Asn2163, both mechanisms could be important, because this residue establishes several interactions with the paratope and also contributes to the stabilization of the short 3_{10} helix forming an N-cap structure.

On the basis of the structural homology between the synthetic peptide and the cognate sequence on VP2, docking studies of the Fab fragment and of the whole 8F5 antibody onto the virion are now in progress.

Structural comparisons between the HRV2 peptide–Fab complex and the unbound Fab fragment

When the unliganded Fab fragment structure of antibody 8F5 (Tormo *et al.*, 1992) is compared with that observed in the presence of the peptide antigen important structural changes, that can be classified in several categories, become apparent.

(i) The elbow angle (defined as the angle formed by the two pseudodyad axes that relate light and heavy chains of the variable and constant modules) has opened from 127° in the uncomplexed Fab structure to 150° in the peptide complex. This change reflects the flexibility of the antibody arms and does not appear to be directly related to the interactions with the ligand, as has been shown for several Fab fragments that have been crystallized with more than one molecule in the asymmetric unit or in different unit cells (Stanfield *et al.*, 1993).

(ii) There is a reorientation in the quaternary association of the variable domains equivalent to a rotation of 3.5°. This kind of movement has been termed interface adaptation (Colman, 1988) and has been shown to contribute significantly to the induced fit mechanism of antigen recognition in several antigen–antibody complexes, the most striking example being the structure of antibody 50.1 complexed with an HIV-1 peptide which presents a rotation of 16.3° (Stanfield *et al.*, 1993). The importance of

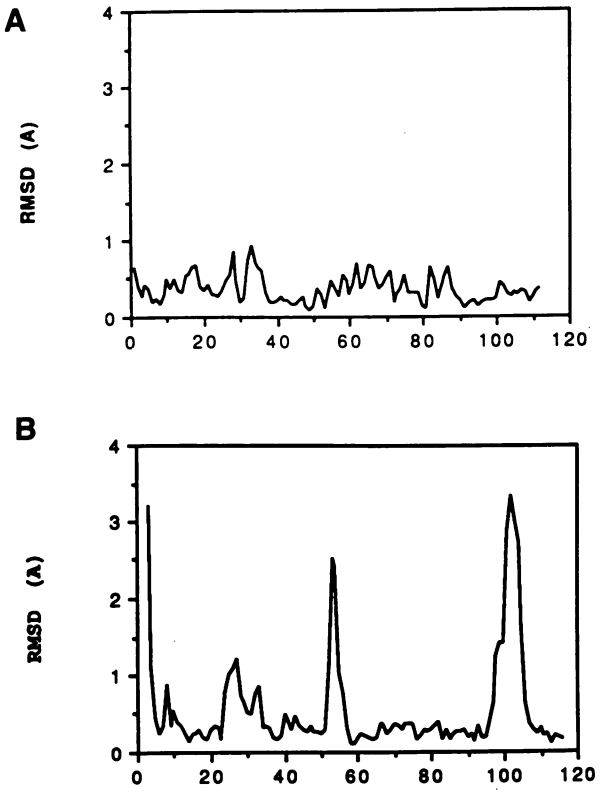

Fig. 6. R.m.s. deviations along the polypeptide sequence between main chain atomic positions of the uncomplexed and the complexed 8F5 Fab fragment structures. In the light chain (**A**) no important differences (<1 Å) are observed (however, the largest displacement is clustered in CDR-L1). In the heavy chain (**B**) residues from the three CDRs show well defined main chain displacements while most of the remaining Fab residues are unchanged. The heavy chain N-terminal residues are disordered in the complex and thus the observed displacements are questionable. The CDR-H3 loop shows the largest changes, in particular atoms from the TyrH102 side chain have a r.m.s. deviation of ~7.5 Å.

reorientation appears to be correlated with the extension of the contact surface between the variable domains. In 8F5 the contact surface area between variable domains is 1316 Å^2 in the unliganded 8F5 Fab and 1290 Å^2 in the complex, well inside the range of values previously reported (from ~1000 Å^2 to 1600 Å^2). Most interface interactions are kept very similar in both 8F5 structures.

(iii) Peptide binding is also accompanied by tertiary conformational changes in the heavy chain CDRs which include displacements of the hypervariable loops and rearrangement of side chains from residues in these regions. Both main chain and side chain atoms show important shifts (Figure 6 and Table III), in particular the r.m.s. displacement for TyrH102(CDR-H3) is >7 Å. On the other hand, the

Table III. Conformational changes around the heavy chain hypervariable loops

Residues[a]	Main chain r.m.s.d.[b]	Side chain r.m.s.d.[b]	Unliganded torsional angles	Liganded torsional angles
CDR-H1				
ThrH24	0.82	2.01	g−	g−
SerH25	1.11	1.17	t	t
GlyH26	1.07	1.40		
PheH27	1.24	2.47	g−	g+
AsnH28	0.95	3.36	g+	t
IleH29	0.84	0.92	t,t	t,t
LysH30	0.70	2.50	g+,t,t	g+,t,g+
AspH31	0.61	1.17	g+	g+
IleH32	0.72	2.05	g−,t	g+,g+
TyrH33	0.72	1.87	g+	g+
CDR-H2				
ArgH50	0.32	1.34	g−,t,t	t,t,t
LeuH51	0.36	0.51	t,g−	t,g−
AspH52	1.05	1.31	t	t
ProH53	2.46	3.42		
AlaH54	2.35	2.61		
AsnH55	0.93	1.83	g+	g−
GlyH56	0.69	0.98		
TyrH57	0.29	0.92	g+	g+
CDR-H3				
AspH97	0.53	1.43	g−	t
GlyH98	1.27	0.85		
TyrH99	1.47	2.27	t	t
TyrH100	1.51	1.65	t	t
SerH101	2.95	3.55	g+	g−
TyrH102	3.47	7.70	t	g+
TyrH103	3.13	3.14	g+	g+
AspH104	2.81	3.94	t	g+
MetH105	1.82	2.75	t,g−,t	g+,t,g−
AspH106	0.76	0.70	t	t
TyrH107	0.41	1.06	g+	g+

[a]Residues that belong to the CDR loops as defined by Kabat *et al.* (1991) are shown in bold type, whereas those that belong to the hypervariable loops as defined by Chothia and Lesk (1987) are in italics.
[b]The average r.m.s. deviations for main chain and side chain atoms, after superposition of the Cα atoms of framework residues as defined by Kabat *et al.* (1991) are shown. Only residues with average deviations for side chain atoms >0.5 Å have been included.

movements of residues in the light chain CDR loops appear to be marginally above average. The displacements of the heavy chain CDR loops can be seen as rigid body rotations which preserve the internal conformation of these loops. In all cases the directions of the shifts are toward the antigen and they result in a reduction of ~3.1% in the volume of the binding site compared with the unliganded structure. CDR-H3 constitutes the hypervariable region which presents a larger displacement upon interaction with the antigen (Figure 6). Furthermore, selected side chains from loops CDR-H2 and especially CDR-H3 have undergone rearrangements in order to optimize their interactions with the antigenic peptide (Table III). TyrH102, which adopted a *trans* conformation for its χ1 torsion angle, pointing away from the antigen binding site in the uncomplexed state, presents a gauche + conformation in the complex. This new conformation allows the formation of a hydrogen bond between the hydroxyl group of TyrH102 and the amide backbone group of Lys2157, as well as several contacts between the aromatic ring and the hydrophobic portion of the side chain of the same residue. However, the orientation of the TyrH102 side chain in the unliganded structure can also be attributed to the interactions, including a hydrogen bond, with a symmetry related molecule in the crystal. In fact, molecular dynamics simulations of the unliganded and complex structures have shown that during the unliganded trajectory the backbone of H3-CDR loop is closer to that observed in the crystal structure of the peptide complex than that of the unbound starting structure which did not include those crystal packing interactions (de la Cruz *et al.*, 1994). These calculations thus suggest that crystal contacts can also influence the orientation of side chains and overall conformation of this, and probably other, hypervariable loops. In the unliganded structure, the carboxyl group of AspH104(CDR-H3)(gauche +) accepted hydrogen bonds from the hydroxyl groups of TyrH99(CDR-H3) and TyrL55(CDR-L2). In the peptide complex, its side chain has flipped upward forming a hydrogen bond with the hydroxyl group of Thr2160 and a salt bridge with Lys2157, whereas the hydroxyl groups of TyrH99(CDR-H3) and TyrL55 (CDR-L2) form hydrogen bonds to solvent molecules.

In CDR-H2 loop only the side chain of residue AsnH55 has changed its orientation from gauche + to gauche −. In the unbound state its side chain amine group donated a hydrogen bond to the carboxylate group of AspH52 in the same loop, whereas in the peptide complex structure these

residues are no longer interacting between them but are involved in hydrogen bonds to backbone groups in the peptide. CDR-H1 loop shows a modest overall displacement, with the more extensive movements and side chain rearrangements in this region located in residues which do not interact with the peptide. These reorientations seem to be related to the shift experimented by CDR-H3. Antibody 8F5 presents a clustering of aromatic side chains from the hypervariable loops CDR-H3 and CDR-H1, facing away from the antigen binding site. The displacement of the backbone of CDR-H3 loop and the flipping of the aromatic ring of TyrH102 in the peptide complex structure are compensated by a rearrangement in the aromatic cluster, a change in the conformation of the phenolic ring of PheH27 and a shift of the polypeptide chain around this residue. This segment of the heavy chain is near to but is not included in the CDR-H1 loop as defined by Kabat *et al.* (1991) and belongs to the hypervariable region as defined by Chothia and Lesk (1987).

(iv) The solvent structure in the vicinity of the recognition pocket also shows important differences. For instance, water molecules replace side chain groups that were forming intramolecular interactions in the unliganded state and are now involved in interactions with the peptide. The side chain of Glu2159 replaces a sulfate ion which is seen in the uncomplexed Fab (Tormo *et al.*, 1992). Some of the water molecules located at the antigen–antibody interface mediate specific interactions.

The concerted combination of all the conformational changes allows the Fab binding site to create a complementary pocket that fits the antigen together with some tightly bound water molecules. In 8F5 the structure of the complex is more compact than the structure of the Fab alone. Thus the accessible surface area for the variable module, decreases from 9096 Å^2 in the unbound 8F5 Fab to 8908 Å^2 in the complex (from this 505 Å^2 correspond to the accessible area on the peptide). The gain in stability for the structure of the complex provides the driving force for the rearrangements observed in this and other Fab studies (Stanfield *et al.*, 1993; Wilson and Stanfield, 1993). However, the plasticity in the paratope and in the whole Fab structure complicates a quantitative description of the mechanisms involved in antigen recognition and the prediction of antibody structures in spite of the achieved efficacy in modeling CDR loops (Chothia and Lesk, 1987; Chothia *et al.*, 1989) and the invariant organization of the antibody framework.

Materials and methods

Crystallization

The production and purification of monoclonal antibody 8F5 and its Fab fragment have been described previously (Tormo *et al.*, 1990). The complex of Fab 8F5 with the 15-mer oligopeptide was crystallized by the hanging-drop vapor diffusion method, using conditions that differ from those which yielded crystals of the unbound Fab fragment (Tormo *et al.*, 1990). Typically, 7 μl droplets containing 7.0 mg/ml of Fab, 1.1 mg/ml of oligopeptide, 0.45 M sodium citrate, 25 mM NaCl, and 50 mM Tris at pH 7.75 were equilibrated against a reservoir containing 1 ml of a solution containing 0.9 M sodium citrate, equally buffered, at 4°C. Crystals grow as prisms which reach sizes ~ 0.7 mm×0.4 mm×0.2 mm in 1–2 months.

Data collection

X-ray diffraction data were collected with a Siemens-Nicolet-Xentronics area detector and nickel-filtered copper K_α radiation from a Rigaku rotating-anode generator, and reduced with the XENGEN program package (Howard *et al.*, 1987). The space group was $P2_12_12_1$, with unit cell dimensions of a = 71.1 Å, b = 75.5 Å and c = 91.4 Å, and one molecule of the complex per asymmetric unit. A data set was obtained from four crystals which was 96.7% complete to 2.5 Å resolution with 93.2% reflections having $F_o > 2\sigma(F_o)$ (79.4% in the 2.6–2.5 Å resolution shell) and an R merge of 0.07 based on intensities. Independently averaged Friedel pairs of the individual crystals had R values between 0.05 and 0.07.

Structure solution and refinement

The structure was determined by molecular replacement (Rossmann, 1972) using the MERLOT package (Fitzgerald, 1988). The starting model was taken from the structure of the uncomplexed Fab fragment of antibody 8F5 which has been solved at 2.8 Å resolution (Tormo *et al.*, 1992). The rotation and translation functions for the variable and constant modules were calculated independently. The model for the variable module comprised residues L1–L112 from the light chain, and residues H1–H116 from the heavy chain, whereas the search model for the constant module was formed by residues L117–L219 and H122–H218. Both models were placed into cubic cells of 100 Å cell length and a B factor of 15 Å^2 was used for all atoms in the structure factor calculation. The fast rotation function (Crowther, 1972) was used with 10.0–4.0 Å resolution data and a radius of integration of 23.9 Å. The rotation search yielded clear peaks for the two modules. The model for the variable module gave a maximum of 7.5σ with the next highest maximum of 4.6σ, whereas the corresponding values for the constant module were 6.8 and 4.7σ, respectively. The Crowther and Blow translation function (Crowther and Blow, 1967) was then used with 10.0–4.0 Å resolution data and the three Harker sections (x = 1/2, y = 1/2, z = 1/2) were examined. Both models provided clear solutions with peaks between 5.9 and 7.4σ; the height of the first spurious peak in each section ranged between 3.5 and 4.1σ. The correctly oriented and positioned models were subjected to rigid body refinement with XPLOR (Brünger, 1990). Initially, the two modules were treated as rigid bodies whereby the R value in the resolution range 8.0–3.0 Å fell from 0.44 to 0.38. During the final cycles the variable heavy, variable light, constant heavy and constant light domains were allowed to move as four separate bodies and the R value dropped to 0.36 in the same resolution range. At this stage, a $2F_o - F_c$ electron density map was calculated. This map clearly showed extra density corresponding to the oligopeptide occupying the antigen binding site. This map also presented poor density for some parts of the three CDRs of the heavy chain that were removed from the model and gradually rebuilt during the course of the refinement. After alternative cycles of least-squares refinement with PROLSQ (Hendrickson, 1985) and manual model building using TOM-FRODO (Jones, 1985; Cambillau and Horjales, 1987) the model was refined to an R value of 24.7% for data between 7.0 and 2.55 Å resolution. A difference electron density map was then used to locate the peptide. The high quality of this electron density allowed us to recognize and build the sequence KAETRLNP. These residues correspond well to the minimal binding site for 8F5. The rest of the peptide did not show clear side chain density and was not built at this stage. After a new round of refinement, the electron densities for residues Val2156 and Asp2165 to Asp2170 were interpretable and they were added to the model. The current R factor for the present model, including ~50 well ordered water molecules, is 17.9% for 15 943 reflections with $F_o > 2\sigma(F_o)$ between 7.0 and 2.50 Å resolution. The r.m.s. deviation for bond lengths is 0.020 Å and for bond angles is 2.3°. The coordinates have been deposited with the Brookhaven Protein Data Bank and will be immediately available.

Acknowledgements

We thank D.Campbell for supplying the peptide, S.Sheriff for providing a modified version of the MS program and J.A.Subirana for encouragement. J.Tormo was recipient of a fellowship from the 'Ministerio de Educación y Ciencia' (Spain). This work was supported by the CICYT (Spain) and the Austrian Bundes-Ministerium für Wissenschaft und Forschung.

References

Alzari,P.M., Lascombe,M.B. and Poljak,R.J. (1988) *Annu. Rev. Immunol.*, **6**, 555–580.

Amzel,L.M. and Poljak,R.J. (1979) *Annu. Rev. Biochem.*, **48**, 961–997.

Appleyard,G., Russell,S.M., Clarke,B.E., Speller,S.A., Trowbridge,M. and Vadolas,J. (1990) *J. Gen. Virol.*, **71**, 1275–1282.

Audibert,F., Jolivet,M., Chedid,L., Arnon,R. and Sela,M. (1982) *Proc. Natl Acad. Sci. USA*, **79**, 5042–5046.

Bjorkman,P.J., Saper,M.A., Samraoui,B., Bennet,W.S., Strominger,J.L.

and Wiley,D.C. (1987) *Nature*, **329**, 506–512.
Brünger,A.T. (1990) *X-PLOR Manual (Version. 2.1)*. Howard Hughes Medical Institute and Department of Molecular Biophysics and Biochemistry, Yale University, New Haven.
Burley,S.K. and Petsko,G.A. (1988) *Adv. Protein Chem.*, **39**, 125–189.
Cambillau,C. and Horjales,E. (1987) *J. Mol. Graphics*, **5**, 174–177.
Case,D.A. and Karplus,M. (1979) *J. Mol. Biol.*, **132**, 343–368.
Chothia,C. and Lesk,A.M. (1987) *J. Mol. Biol.*, **196**, 901–917.
Chothia,C. *et al.* (1989) *Nature*, **342**, 877–883.
Colman,P.M. (1988) *Adv. Immunol.*, **43**, 99–132.
Connolly,M.L. (1983) *J. Appl. Crystallogr.*, **16**, 548–558.
Crowther,R.A. (1972) In Rossmann,M.G. (ed.), *The Molecular Replacement Method*. Gordon and Breach, New York, pp. 173–178.
Crowther,R.A. and Blow,D.M. (1967) *Acta Crystallogr.*, **23**, 544–548.
Davies,D.R., Padlan,E.A. and Sheriff,S. (1990) *Annu. Rev. Biochem.*, **59**, 439–473.
de la Cruz,X., Mark,A.E., Tormo,J., Fita,I. and van Gunsteren,W. (1994) *J. Mol. Biol.*, **236**, 1186–1195.
Dimmock,N.J. (1993) *Neutralization of Animal Viruses*. Springer Verlag, Berlin.
Fitzgerald,P.M.D. (1988) *J. Appl. Crystallogr.*, **21**, 273–278.
Francis,M.J., Hastings,G.Z., Sangar,D.V., Clark,R.P., Syred,A., Clarke,B.E., Rowlands,D.J. and Brown,F. (1987) *J. Gen. Virol.*, **68**, 2687–2691.
Garcia,K.C., Ronco,P.M., Verroust,P.J., Brünger,A.T. and Amzel,L.M. (1992) *Science*, **257**, 502–507.
Geysen,H.M., Rodda,S.J., Mason,T.J., Tribbick,G. and Schoofs,P.G. (1987) *J. Immunol. Methods*, **102**, 259–274.
Hastings,G.Z., Speller,S.A. and Francis,M.J. (1990) *J. Gen. Virol.*, **71**, 3055–3059.
Hendrickson,W.A. (1985) *Methods Enzymol.*, **115**, *252–270.*
Howard,A.J., Gilliland,G.L., Finzel,B.C. and Poulos,T.L. (1987) *J. Appl. Crystallogr.*, **20**, 383.
Jacob,C.O., Pines,M. and Arnon,R. (1984) *EMBO J.*, **3**, 2889–2893.
Javaherian,K., Langlois,A.J., LaRosa,G.J., Profy,A.T., Bolognesi,D.P., Herlihy,W.C., Putney,S.D. and Mathews,T.J. (1990) *Science*, **250**, 1590–1593.
Jones,T.A. (1985) *Methods Enzymol.*, **115**, 157–171.
Jones,T.A., Zou,J.-Y., Cowan,S.W. and Kjeldgaard,M. (1991) *Acta Crystallogr.*, **A47**, 110–119.
Kabat,E.A., Wu,T.T., Reid-Miller,M., Perry,H.M. and Gottesman,K.S. (1991) *Sequences of Proteins of Immunological Interest*. 5th edn. National Institutes of Health, Bethesda MD.
Kim,S., Smith,T.J., Chapman,M.S., Rossmann,M.G., Pevear,D.C., Dutko,F.J., Felock,P.J., Diana,G.D. and McKinlay,M.A. (1989) *J. Mol. Biol.*, **210**, 91–111.
Mian,I.S., Bradwell,A.R. and Olson,A.J. (1991) *J. Mol. Biol.*, **217**, 133–151.
Muller,G.M., Shapira,M. and Arnon,R. (1982) *Proc. Natl Acad. Sci. USA*, **79**, 569–573.
Olson,N.H., Kolatkar,P.R., Oliveira,M.A., Cheng,R.H., Greve,J.M., McClelland,A., Baker,T.S. and Rossmann,M.G. (1993) *Proc. Natl Acad. Sci. USA*, **90**, 507–511.
Padlan,E.A. (1990) *Proteins*, **7**, 112–124.
Parry,N.R., Barnet,P.V., Ouldridge,E.J., Rowlands,D.J. and Brown,F. (1989) *J. Gen. Virol.*, **70**, 1493–1503.
Patarroyo,M.E. *et al., (1988) Nature*, **332**, 158–161.
Prasad,B.V.V., Burns,J.W., Marietta,E., Estes,M.K. and Chiu,W. (1990) *Nature*, **343**, 476–479.
Richardson,J.S. (1981) *Adv. Protein Chem.*, **34**, 167–339.
Rini,J.M., Schulze-Gahmen,U. and Wilson,I.A. (1992) *Science*, **255**, 959–965.
Rini,J.M., Stanfield,R.L., Stura,E.A., Salinas,P.A., Profy,A.T. and Wilson,I.A. (1993) *Proc. Natl. Acad. Sci. USA.*, **90**, 6325–6329.
Rossmann,M.G. (1972) *The Molecular Replacement Method*. Gordon and Breach, New York.
Rossmann,M.G. and Johnson,J.E. (1989) *Annu. Rev. Biochem.*, **58**, 533–573.
Rossmann,M.G. *et al.* (1985) *Nature*, **317**, 145–153.
Sheriff,S., Hendrickson,W.A. and Smith,J.L. (1987) *J. Mol. Biol.*, **197**, 273–296.
Skern,T., Neubauer,C., Frasel,L., Gründler,P., Sommergruber,W., Zorn,M., Kuechler,E. and Blaas,D. (1987) *J. Gen. Virol.*, **68**, 315–323.
Smith,T.J., Olson,N.H., Cheng,R.H., Liu,H., Chase,E.S., Lee,W.M., Leippe,D.M., Mosser,A.G., Rueckert,R.R. and Baker,T.S. (1993) *J. Virol.*, **67**, 1148–1158.
Stanfield,R.L., Fieser,T.M., Lerner,R.A. and Wilson,I.A. (1990) *Science*, **248**, 712–719.
Stanfield,R.L., Takimoto-Kamimura,M., Rini,J.M., Profy,A.T. and Wilson,I.A. (1993) *Structure*, **1**, 83–93.
Tormo,J., Fita,I., Kanzler,O. and Blaas,D. (1990) *J. Biol. Chem.*, **265**, 16799–16800.
Tormo,J., Stadler,E., Skern,T., Auer,H., Kanzler,O., Betzel,C., Blaas,D. and Fita,I. (1992) *Protein Sci.*, **1**, 1154–1161.
Van Regenmortel,M.H.V. (1989) *Immunol. Today*, **10**, 266–272.
Vix,O., Rees,B., Thierry,J.C. and Altschuh,D. (1993) *Proteins*, **15**, 339–348.
Wang,G., Porta,C., Chen,Z., Baker,T.S. and Johnson,J.E. (1992) *Nature*, **355**, 275–278.
Wilmot,C.M. and Thornton,J.M. (1990) *Protein Engng*, **3**, 479–493.
Wilson,I.A. and Stanfield,R.L. (1993) *Curr. Opin. Struct. Biol.*, **3**, 113–118.

Received on July 26, 1993; revised on February 7, 1994